

Optimal Low-Thrust Transfer in General Circular Orbit Using Analytic Averaging of the System Dynamics¹

Jean A. Kéchichian²

Abstract

Edelbaum's classic problem of minimum-time low-thrust transfer between inclined circular orbits is analyzed within the context of the additional perturbation due to the Earth's oblateness. The original analytic theory using only the orbital velocity V and relative inclination i variables, which is sufficient to describe the transfers between conic orbits, is extended by also considering the right ascension of the ascending node Ω variable needed to account for the precession of the instantaneous orbit during the transfer due to the second zonal harmonic J_2 perturbation. Analytic averaging of the dynamic and adjoint differential equations using a piecewise constant thrust angle is carried out for the thrust-perturbation-only case within the framework of the three-state description above in order to emulate the purely closed-form Edelbaum solution. For the more general precessed orbit plane case, an identical analytic averaging is carried out to rotate the orbit plane around the instantaneous line of nodes to generate the set of averaged differential equations that do not require numerical quadratures during their integration. The suboptimal results are compared to the purely numerical solutions using precision integration on a four-state system description by the addition of the mean angular position α as the fourth state variable with continuously varying thrust vector orientation for the unaveraged system dynamics, and additionally using numerical quadrature for the averaged system dynamics case.

Introduction

The analysis of optimal low-thrust orbit transfer between circular orbits of general size and orientation has benefitted from several contributions in references [1–5]. In particular Edelbaum provided in reference [1] his classical analytic expression for the velocity change or ΔV needed to transfer between two circles of uneven size and relative inclination in minimum-time while applying continuous constant thrust

¹Presented at the F. Landis Markley Astronautics Symposium, Cambridge, Maryland, June 29–July 2, 2008.

²Engineering Specialist, Astrodynamics Department, The Aerospace Corporation, MS M4/946, P. O. Box 92957, Los Angeles, CA 90009. E-mail: Jean.A.Kechichian@aero.org. Copyright ©2008 by The Aerospace Corporation.

acceleration. In the absence of the Earth oblateness effect due mainly to the harmonic J_2 , it is convenient to consider the relative inclination of one orbit with respect to the other and thus ignore the right ascension of the ascending node Ω in the system of dynamic equations which reduces then to only two states, namely, the orbital velocity V and the relative inclination i . The differential equations in V and i can be averaged by considering a simple thrust vectoring strategy which essentially holds the thrust angle piecewise-constant during each revolution, switching signs at the antinodes. The angular position can thereby be removed from these dynamic equations enabling a closed-form solution for the state variables V and i as a function of time.

Transfer examples are also analyzed in reference [6] and the use of equinoctial elements in general transfers between any elliptic or circular orbits was introduced first in reference [7]. This author has also provided several contributions to solve the general problem using various sets of nonsingular elements. This paper concentrates on the important circular application and assumes that the instantaneous orbit remains circular during the transfer such that the problem can be further investigated using a reduced set of dynamic variables instead of the full six-state system needed in the more general elliptic transfer.

Typical long duration precision integration transfers spanning several months with the full six-state dynamics and continuous thrust vectoring from LEO to GEO stay essentially circular. It is only when high accelerations are used resulting in fast sub-day transfers that the intermediate orbits' eccentricities can be substantial not unlike the impulsive GTO case. The analytic Edelbaum ΔV estimates for LEO to GEO transfers are only less than 3% higher than their exact counterparts and the transfers are much easier to implement in an operational sense.

In a first analysis, the general circular problem is revisited in the absence of any oblateness-induced perturbation by considering the three states V , i and Ω and by also using the piecewise-constant thrust yaw assumption in order to arrive at a system of averaged equations which can be solved numerically. The results must then mimic Edelbaum's findings. An unaveraged dynamic system using this time all four states including the mean angular position α defined in the next section, and continuously orienting the thrust vector along the instantaneous optimal direction is also solved numerically for comparison purposes and in preparation to include the important J_2 perturbation. The J_2 perturbation is then accounted for both in the "exact" or unaveraged sense with optimal thrust vectoring, and within the context of an analytic averaging that uses the piecewise-constant yaw strategy mentioned earlier. However unlike the thrust-only problem, the addition of J_2 will precess the orbit plane and start to vary the orientation of the line of nodes which effectively stayed fixed in the thrust-only problem. Therefore the instantaneous line of nodes must be continuously updated to continue the process of analytic averaging in a reliable manner. Numerical comparisons are provided with the "exact" solution that does not average out the angular position which in turn makes the search for the "exact" solutions more difficult as discussed in the text.

The Analytic Averaging of the Three-State Dynamics for the Thrust-Only Case (i^* Theory)

In this section, Edelbaum's analytic description of the circle-to-inclined-circle transfer using only the orbital velocity V and relative inclination i , is reformulated within the context of the three-state dynamics description with the right ascension

of the ascending node Ω as the third state variable. In the absence of the J_2 perturbation, it is convenient to assume that the initial orbit plane is effectively the equatorial plane such that the relative inclination of the final orbit respective to the initial orbit represents effectively the equatorial inclination angle itself. Thus, it is sufficient to consider only the state variables V and i .

Starting from the full set of the Gaussian form of the Lagrange planetary equations for near-circular orbits, namely

$$\frac{da}{dt} = 2af_i/V \quad (1)$$

$$\frac{de_x}{dt} = 2f_t c_\alpha/V - f_n s_\alpha/V \quad (2)$$

$$\frac{de_y}{dt} = 2f_t s_\alpha/V + f_n c_\alpha/V \quad (3)$$

$$\frac{di}{dt} = f_h c_\alpha/V \quad (4)$$

$$\frac{d\Omega}{dt} = f_h s_\alpha/(Vs_i) \quad (5)$$

$$\frac{d\alpha}{dt} = n + 2f_n/V - f_h s_\alpha/(V \tan i) \quad (6)$$

where s_α and c_α stand for $\sin \alpha$ and $\cos \alpha$ with $\alpha = \omega + M$ standing for the mean angular position given in terms of the classical elements, a the orbit semimajor axis, and $e_x = ec_\omega$, $e_y = es_\omega$ replacing e and ω with the latter poorly defined in near-circular orbit. The mean motion is given by $n = (\mu/a^3)^{1/2}$ with μ the Earth gravity constant, and the thrust acceleration \mathbf{f} resolved along the tangent, normal and out-of-plane directions given by f_t , f_n , and f_h with the normal direction oriented towards the center of attraction. Assuming only tangential and out-of-plane acceleration, i.e., letting $f_n = 0$, and assuming the orbit remains circular during the transfer, and letting β represent the thrust yaw angle such that $f_t = fc_\beta$ and $f_h = fs_\beta$, and letting $\alpha = \omega + M = \omega + \theta^* = \theta$ because $e = 0$, with $\theta = nt$ and θ^* the true anomaly, the original differential equations (1–6) are further reduced to the form

$$\frac{da}{dt} = 2af_i/V \quad (7)$$

$$\frac{di}{dt} = c_\theta f_h/V \quad (8)$$

$$\frac{d\Omega}{dt} = s_\theta f_h/(Vs_i) \quad (9)$$

$$\frac{d\theta}{dt} = n - s_\theta f_h/(V \tan i) \quad (10)$$

The assumption $f_n = 0$ is validated by the observation that circle-to-circle transfers remain essentially circular as discussed above.

Letting β be a piecewise constant switching sign at the orbital antinodes, the $s_\theta f_h$ terms will give zero contribution such that equation (10) is replaced by

$$\frac{d\theta}{dt} = n \quad (11)$$

Averaging out the angle θ and in view of $V = na = (\mu/a)^{1/2}$, the averaged system equations reduce to the form

$$\dot{\bar{i}} = \frac{1}{2\pi} \int_0^{2\pi} \left(\frac{di}{dt} \right) d\theta = \frac{2fs_\beta}{2\pi V} \int_{-\pi/2}^{\pi/2} c_\theta d\theta = \frac{2fs_\beta}{\pi V} \quad (12)$$

$$\dot{\bar{V}} = -fc_\beta \quad (13)$$

$$\dot{\bar{\Omega}} = \frac{1}{2\pi} \int_0^{2\pi} \left(\frac{d\Omega}{dt} \right) d\theta = \frac{2fs_\beta}{2\pi Vs_i} \int_{-\pi/2}^{\pi/2} s_\theta d\theta = 0 \quad (14)$$

The transfer can now be analyzed using only the \tilde{V} , \tilde{i} variables leading to the analytic solutions in [1], [2], [4] and [5]. When the three-state system is considered, the orbit inclination is relative to the equator as shown in Fig. 1 where the initial and final orbits' orientations are described by the (i_1, Ω_1) and (i_2, Ω_2) pairs with θ_i and θ_f the angular positions of the relative node at A, and i_{tot}^* the total relative inclination.

Holding β piecewise constant with sign change at the antinodes of the relative node at A, the averaged equations are now given by

$$\dot{\tilde{V}} = -fc_\beta \quad (15)$$

$$\dot{\tilde{i}} = \frac{1}{2\pi} \int_0^{2\pi} \left(\frac{di}{dt} \right) d\theta = \frac{2fs_\beta}{2\pi V} \int_{\theta_c - \pi/2}^{\theta_c + \pi/2} c_\theta d\theta = \frac{2fs_\beta}{\pi V} c_{\theta_c} \quad (16)$$

$$\dot{\tilde{\Omega}} = \frac{1}{2\pi} \int_0^{2\pi} \left(\frac{d\Omega}{dt} \right) d\theta = \frac{2fs_\beta}{2\pi Vs_i} \int_{\theta_c - \pi/2}^{\theta_c + \pi/2} s_\theta d\theta = \frac{2fs_\beta}{\pi Vs_i} s_{\theta_c} \quad (17)$$

where θ_c is the instantaneous angular position of A, sweeping the interval θ_i , θ_f during the transfer, while the relative inclination i^* sweeps the interval i_{tot}^* , 0. As in the original two-state theory, the angle β can now be considered to be a continuous quantity even though in practice it must change its value from one orbit to the next while holding it constant inside each revolution. The relative line of nodes stays

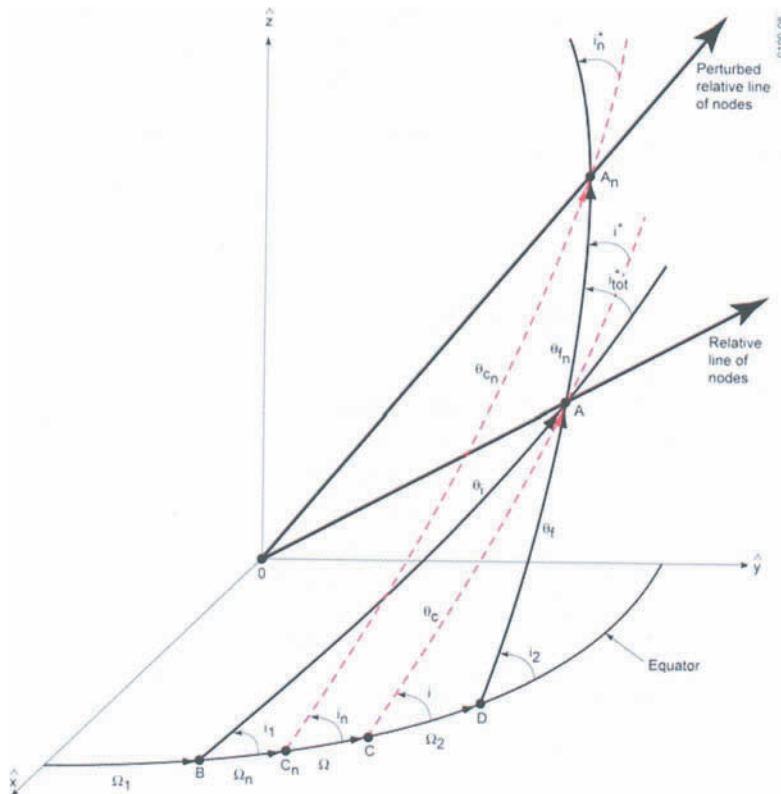


FIG. 1. Orbit Geometry.

fixed in space even though the orbit size is continuously changing during the transfer. From spherical trigonometry we have

$$c_{i_{tot}}^* = c_{\Omega_1 - \Omega_2} s_{i_1} s_{i_2} + c_{i_1} c_{i_2} \quad (18)$$

The angles θ_i and θ_f are also computed from

$$s_{\theta_i} = s_{i_2} s_{\Omega_2 - \Omega_1} / s_{i_{tot}}^* \quad (19)$$

$$c_{\theta_i} = (c_{i_{tot}}^* c_{i_1} - c_{i_2}) / (s_{i_{tot}}^* s_{i_1}) \quad (20)$$

$$s_{\theta_f} = s_{i_1} s_{\Omega_2 - \Omega_1} / s_{i_{tot}}^* \quad (21)$$

$$c_{\theta_f} = (c_{i_1} - c_{i_2} c_{i_{tot}}^*) / (s_{i_2} s_{i_{tot}}^*) \quad (22)$$

The instantaneous i^* angle is then given by

$$s_{i^*} = s_{\Omega_2 - \Omega} s_i / s_{\theta_f} \quad (23)$$

$$c_{i^*} = c_{i_1} c_{i_2} + s_{i_1} s_{i_2} c_{\Omega_2 - \Omega} \quad (24)$$

and it can be extracted directly and without ambiguity from equation (24) because $0 \leq i^* \leq \pi$.

Finally the angle θ_c is given by

$$s_{\theta_c} = s_{i_2} s_{\theta_f} / s_i \quad (25)$$

$$c_{\theta_c} = c_{\Omega_2 - \Omega} c_{\theta_f} - s_{\Omega_2 - \Omega} s_{\theta_f} c_{i_2} \quad (26)$$

This angle is continuously updated during the numerical integration of the averaged system in equations (15–17). All variables are thus considered to be averaged values. The minimum-time solution requires the generation of the adjoint or multipliers differential equations for $\tilde{\lambda}_V$, $\tilde{\lambda}_i$ and $\tilde{\lambda}_\Omega$ obtained from the averaged Hamiltonian \tilde{H} given by

$$\tilde{H} = 1 + \tilde{\lambda}_V \dot{V} + \tilde{\lambda}_i \dot{i} + \tilde{\lambda}_\Omega \dot{\Omega} = 1 - \tilde{\lambda}_V f c_\beta + \tilde{\lambda}_i \left(\frac{2f s_\beta}{\pi V} c_{\theta_c} \right) + \tilde{\lambda}_\Omega \left(\frac{2f s_\beta}{\pi V s_i} s_{\theta_c} \right) \quad (27)$$

such that

$$\dot{\tilde{\lambda}}_V = -\partial \tilde{H} / \partial V = \frac{2f s_\beta}{\pi V^2} \left(\tilde{\lambda}_i c_{\theta_c} + \frac{\tilde{\lambda}_\Omega}{s_i} s_{\theta_c} \right) \quad (28)$$

$$\dot{\tilde{\lambda}}_i = -\partial \tilde{H} / \partial i = \tilde{\lambda}_\Omega \frac{2f s_\beta}{\pi V} \frac{c_i}{s_i^2} s_{\theta_c} \quad (29)$$

$$\dot{\tilde{\lambda}}_\Omega = -\partial \tilde{H} / \partial \Omega = 0 \quad (30)$$

The optimal thrust yaw angle β is obtained from the optimality condition

$$\partial \tilde{H} / \partial \beta = \tilde{\lambda}_V f s_\beta + \tilde{\lambda}_i \frac{2f c_\beta}{\pi V} c_{\theta_c} + \tilde{\lambda}_\Omega \frac{2f c_\beta}{\pi V s_i} s_{\theta_c} = 0 \quad (31)$$

An anonymous reviewer of this paper has suggested that the strengthened Legendre-Clebsch condition $\partial^2 \tilde{H} / \partial \beta^2 > 0$, which is a second-order condition for a local minimum, can be satisfied by the local minimum ensuring thrust direction given by $c_\beta = a(a^2 + b^2)^{-1/2}$, $s_\beta = -b(a^2 + b^2)^{-1/2}$ because $\partial \tilde{H} / \partial \beta$ has the form $a s_\beta + b c_\beta$.

Equation (31) leads to

$$\tan \beta = - \left(\tilde{\lambda}_i c_{\theta_c} + \frac{\tilde{\lambda}_\Omega}{s_i} s_{\theta_c} \right) \frac{2}{\pi V \tilde{\lambda}_V} = \frac{s_\beta}{c_\beta} \quad (32)$$

Given initial V_0 , i_0 , Ω_0 and final V_f , i_f , Ω_f and a thrust acceleration magnitude f , the two-point-boundary-value-problem is solved by guessing the initial values of the multipliers as well as the total flight time t_f and integrating the system equations (15–17) and adjoint equations (28–30) using the optimal thrust angle β given in equation (32), from time zero, i.e., t_0 until t_f , and iterating on the guessed values until V_f , i_f , Ω_f as well as $H_f = 0$ are satisfied.

Note that the Hamiltonian \tilde{H} is not constant here even though it is not an explicit function of time because of the formulation that involves the angle θ_c . Even though the relative line of nodes remains fixed in space, the angle θ_c varies from θ_i to θ_f during the transfer such that

$$\frac{d\tilde{H}}{dt} = \frac{\partial \tilde{H}}{\partial t} + \frac{\partial \tilde{H}}{\partial \tilde{x}} \dot{\tilde{x}} + \frac{\partial \tilde{H}}{\partial \tilde{\lambda}} \dot{\tilde{\lambda}} + \frac{\partial \tilde{H}}{\partial \theta_c} \dot{\theta}_c = \frac{\partial \tilde{H}}{\partial \theta_c} \dot{\theta}_c \neq 0$$

Because $\partial \tilde{H}/\partial t = 0$ and $\partial \tilde{H}/\partial \tilde{x} = -\dot{\tilde{\lambda}}$, $\partial \tilde{H}/\partial \tilde{\lambda} = \dot{\tilde{x}}$. However, if we replace c_{θ_c} and s_{θ_c} by their expressions as functions of $\tilde{\Omega}$ and \tilde{i} then $\dot{\tilde{\lambda}}_v = -\partial \tilde{H}/\partial \tilde{V}$ remains unchanged, while $\dot{\tilde{\lambda}}_\Omega = -\partial \tilde{H}/\partial \tilde{\Omega}$ and $\dot{\tilde{\lambda}}_i = -\partial \tilde{H}/\partial \tilde{i}$ will have a different form and the Hamiltonian \tilde{H} will be effectively constant, with $\tan \beta$ also unchanged. The Hamiltonian \tilde{H} decreases from 0.14249 at time zero to essentially zero at t_f for the example shown in the next section.

Precision Integration Optimization Using the Four-State System

Going back to equations (7–10), and in view of $n = V^3/\mu$ in circular orbit, and once again using only the $f_i = fc_\beta$ and $f_h = fs_\beta$ accelerations we have the four-state dynamic equations given by

$$\dot{V} = -fc_\beta \quad (33)$$

$$\dot{i} = fs_\beta c_a/V \quad (34)$$

$$\dot{\Omega} = fs_\beta s_a/(Vs_i) \quad (35)$$

$$\dot{\alpha} = V^3/\mu - fs_\beta s_a/(V \tan i) \quad (36)$$

For minimum-time solutions, the Hamiltonian of the system reads as

$$\begin{aligned} H = 1 + \lambda_V \dot{V} + \lambda_i \dot{i} + \lambda_\Omega \dot{\Omega} + \lambda_\alpha \dot{\alpha} &= 1 + \lambda_V (-fc_\beta) + \lambda_i \left(\frac{fs_\beta c_\alpha}{V} \right) \\ &+ \lambda_\Omega \left(\frac{fs_\beta s_\alpha}{Vs_i} \right) + \lambda_\alpha \left(\frac{V^3}{\mu} - \frac{fs_\beta s_\alpha}{V \tan i} \right) \end{aligned} \quad (37)$$

This leads to the multipliers equations as

$$\dot{\lambda}_V = -\frac{\partial H}{\partial V} = \lambda_i \frac{fs_\beta c_\alpha}{V^2} + \lambda_\Omega \frac{fs_\beta s_\alpha}{V^2 s_i} - \lambda_\alpha \left(\frac{3V^2}{\mu} \right) - \lambda_\alpha \frac{fs_\beta s_\alpha}{V^2 \tan i} \quad (38)$$

$$\dot{\lambda}_i = -\frac{\partial H}{\partial i} = \lambda_\Omega \frac{fs_\beta s_\alpha c_i}{Vs_i^2} - \lambda_\alpha \frac{fs_\beta s_\alpha}{Vs_i^2} \quad (39)$$

$$\dot{\lambda}_\Omega = -\frac{\partial H}{\partial \Omega} = 0 \quad (40)$$

$$\dot{\lambda}_\alpha = -\frac{\partial H}{\partial \alpha} = \lambda_i \frac{fs_\beta s_\alpha}{V} - \lambda_\Omega \frac{fs_\beta c_\alpha}{Vs_i} + \lambda_\alpha \frac{fc_\beta c_\alpha}{V \tan i} \quad (41)$$

The thrust yaw angle β is obtained from the optimality condition

$$\frac{\partial H}{\partial \beta} = \lambda_V fs_\beta + \lambda_i \frac{fc_\beta c_\alpha}{V} + \lambda_\Omega \frac{fc_\beta s_\alpha}{Vs_i} - \lambda_\alpha \frac{fc_\beta s_\alpha}{V \tan i} = 0 \quad (42)$$

leading to

$$\tan \beta = \frac{-\lambda_i \frac{c_\alpha}{V} - \lambda_\Omega \frac{s_\alpha}{Vs_i} + \lambda_\alpha \frac{s_\alpha}{V \tan i}}{\lambda_V} = \frac{s_\beta}{c_\beta} \quad (43)$$

In order to find the overall minimum-time solution for transfer between given initial and final states, namely V_0, i_0, Ω_0 and V_f, i_f, Ω_f it is necessary to optimize the initial and final locations on the initial and final orbits respectively, instead of selecting them arbitrarily. The optimal solution therefore requires that $(\lambda_\alpha)_0 = (\lambda_\alpha)_f = 0$. Thus, given $V_0, i_0, \Omega_0, (\lambda_\alpha)_0 = 0$, and $V_f, i_f, \Omega_f, (\lambda_\alpha)_f = 0$, the initial values $(\lambda_V)_0, (\lambda_i)_0, (\lambda_\Omega)_0, (\alpha)_0$ as well as t_f are guessed and the state and adjoint equations (33–36) and (38–41) are integrated forward from $t_0 = 0$ until t_f using the optimal firing angle β in equation (43). The guessed values are adjusted by an optimizer program until $V_f, i_f, \Omega_f, (\lambda_\alpha)_f = 0$ and $H_f = 0$ are closely matched within a small tolerance.

The following example is now used to generate the relevant optimal transfers, namely $a_0 = 6563.14$ km, $V_0 = 7.7931587$ km/s, $i_0 = 10$ deg, $\Omega_0 = 20$ deg, $a_f = 6878$ km, corresponding to $V_f = 7.6126921$ km/s, $i_f = 5$ deg, $\Omega_f = 10$ deg, with $f = 3.5 \times 10^{-6}$ km/s². Because the Hamiltonian system is homogeneous in the multipliers, we can scale the initial values of the multipliers in order to get $H_f = -1$ instead of $H_f = 0$ provided that $H = \lambda^T \dot{x}$ is used instead of $H = 1 + \lambda^T \dot{x}$. In this precision-integrated four-state system, $H_f = -1$ is thereby enforced as a boundary condition. Also, H is a constant of the motion, not being an explicit function of time. Table 1 below shows the solutions obtained via the four-state theory as well as those from the three-state i^* theory of the first section and the purely analytic Edelbaum theory in [1], [4]. The two-state V, i analytic theory requires the computation of the single relative inclination change i^* directly obtained from the V_0, i_0 and V_f, i_f pairs through equation (18). Thus $(\lambda_i)_0$ effectively stands for $(\lambda_{i^*})_0$ in the analytic theory.

In the Edelbaum run, i^* goes from 0 to 5.148939835 deg instead of the other way around such that $(\lambda_i)_0$ has the opposite sign with respect to the $(\lambda_i)_0$ of the other two theories.

Table 2 below shows the initial and final parameters for the three cases. The $(\alpha)_0$ and $(\alpha)_f$ angular positions are optimized such that they represent the departure and arrival locations on the initial and final orbits. Also $(\lambda_\alpha)_f = 0$ is matched closely as a boundary condition, while $H_f = 0$ instead of $H_f = -1$ are enforced for the three-state and four-state cases. The β angle history for the three cases is shown in Fig. 2, with the analytic and averaged curves being essentially identical because β must switch sign at each antinode to mimic the oscillation of the exact solution.

TABLE 1. Solutions From the Three-State-Averaged, Four-State Precision-Integrated and the Analytic Edelbaum Theories

	$(\lambda_v)_o$ (s/km/s)	$(\lambda_i)_o$ (s/rad)	$(\lambda_a)_o$ (s/rad)	t_f (s)	ΔV (km/s)
Three-state-averaged	0.5915208891×10^5	0.2547555258×10^7	0.4112381940×10^6	3.146527652×10^5	1.1012846
Four-state-unaveraged	0.162483798×10^5	0.240312782×10^7	0.071394913×10^6	3.12638781×10^5	1.09442357
Analytic Edelbaum	0.6646589168×10^5	$-0.3401606421 \times 10^7$	N/A	3.146467816×10^5	1.1012637

TABLE 2. Initial and Final Achieved Parameters

	V_0 (km/s) V_f (km/s)	i_0 (deg) i_f (deg)	Ω_0 (deg) Ω_f (deg)	α_0 (deg) α_f (deg)	$(\lambda_a)_0$ (s/rad) $(\lambda_a)_f$ (s/rad)	H_f
Three-state-averaged	7.7931587 7.6126921	10.0 5.00000074	20.0 10.0	10.00000030 20.0	345.4613991 46.85238677	6.2246×10^{-9}
Four-state-unaveraged	7.7931587 7.6127009	10.0 4.999983319	20.0 9.999944152	345.4613991 46.85238677	0.0 3.49414×10^{-6}	-0.9999785801
Analytic Edelbaum	7.7931587 7.6126921	$i_f^* = 1.590277 \times 10^{-15}$ $i_0^* = 5.148939835$			-1.78258×10^{-17}	

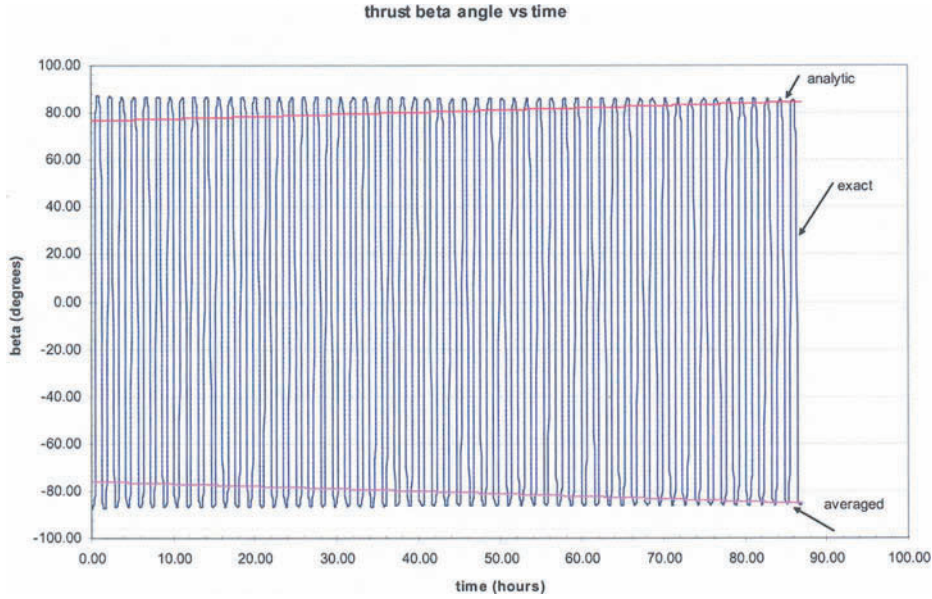


FIG. 2. Thrust β Angle History for the Averaged, Exact and Edelbaum Theories.

The analytic and averaged β curves have opposite signs because i^* goes from 0 to 5.148939835 deg as mentioned earlier. However the two curves are essentially identical. Figure 3 shows the velocity evolutions with a small oscillatory behavior in the exact case, while Figs. 4 and 5 show the inclination and node depictions.

Precision Integration Optimization Using the Four-State System Under J_2 Influence

It is well known that the components of the J_2 acceleration along the axes of the rotating Euler-Hill frame ($\hat{\mathbf{r}}, \hat{\boldsymbol{\theta}}, \hat{\mathbf{h}}$) can be written as (for the circular orbit case in view of $r^4 = \mu^4/V^8$ because $V^2 = \mu/r = \mu/a$)

$$(f_r)_{J_2} = -\frac{3\mu J_2 R^2}{2r^4} (1 - 3s_i^2 s_\theta^2) = -\frac{3J_2 R^2}{2\mu^3} V^8 (1 - 3s_i^2 s_\theta^2) \quad (44)$$

$$(f_\theta)_{J_2} = -\frac{3\mu J_2 R^2}{r^4} s_i^2 s_\theta c_\theta = -\frac{3J_2 R^2}{\mu^3} V^8 s_i^2 s_\theta c_\theta \quad (45)$$

$$(f_h)_{J_2} = -\frac{3\mu J_2 R^2}{r^4} s_i c_i s_\theta = -\frac{3J_2 R^2}{\mu^3} V^8 s_i c_i s_\theta \quad (46)$$

In equations (44–46), R stands for the radius of the equator and $(f_r)_{J_2} = -(f_h)_{J_2}$ and $(f_i)_{J_2} = (f_\theta)_{J_2}$ for the circular case. Going back to equations (1), (4–6) we have with $\alpha = \theta$, from $\dot{a} = 2af_i/V$

$$\dot{V} = -[(f_i)_T + (f_i)_{J_2}] = -fc_\beta - (f_\theta)_{J_2} = -fc_\beta + \frac{3J_2 R^2}{\mu^3} V^8 s_i^2 s_\alpha c_\alpha \quad (47)$$

$$i = [(f_h)_T + (f_h)_{J_2}] \frac{c_\alpha}{V} = \frac{fs_\beta c_\alpha}{V} - \frac{3J_2 R^2}{\mu^3} V^7 s_i c_i s_\alpha c_\alpha \quad (48)$$

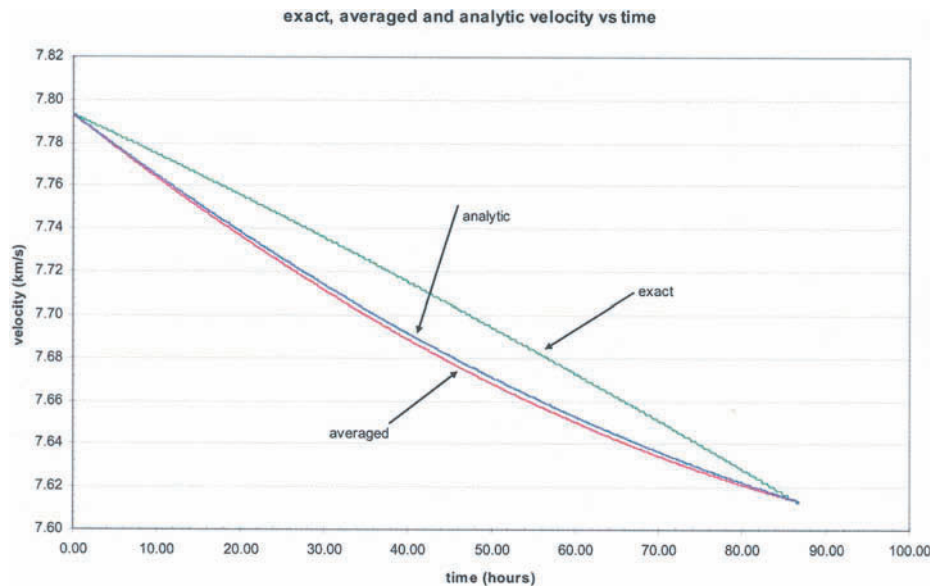


FIG. 3. Evolution of Orbital Velocity for the Averaged, Exact and Edelbaum Theories.

$$\dot{\Omega} = [(f_h)_T + (f_h)_{J_2}] \frac{s_\alpha}{V s_i} = \frac{f s_\beta s_\alpha}{V s_i} - \frac{3 J_2 R^2}{\mu^3} V^7 c_i s_\alpha^2 \quad (49)$$

$$\dot{\alpha} = n - \frac{2(f_h)_{J_2}}{V} - \frac{(f_h)_T s_\alpha}{V \tan i} - \frac{(f_h)_{J_2} s_\alpha}{V \tan i} = \frac{V^3}{\mu} + \frac{3 J_2 R^2 V^7}{\mu^3} [1 + s_\alpha^2 (1 - 4 s_i^2)] - \frac{f s_\beta s_\alpha}{V \tan i} \quad (50)$$

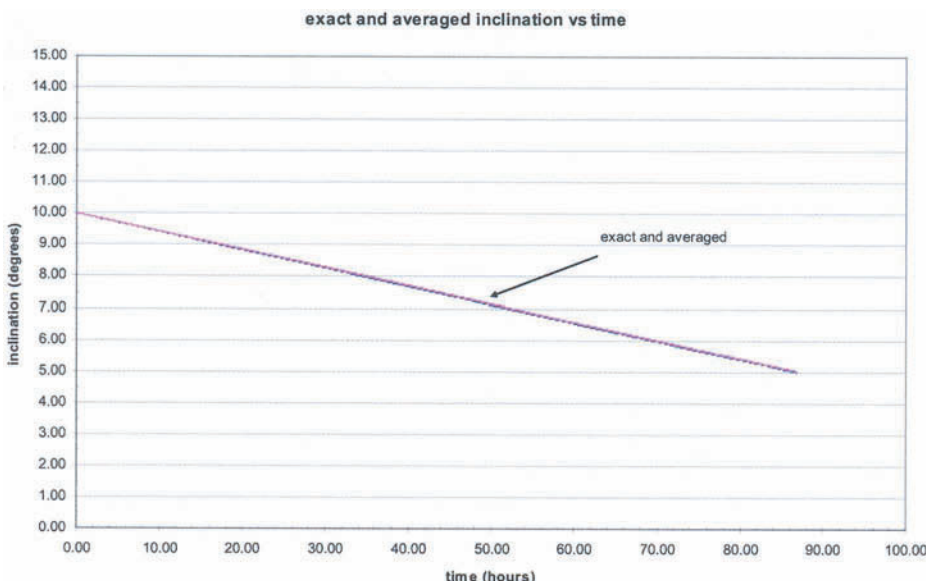


FIG. 4. Evolution of Orbital Inclination for the Averaged and Exact Theories.

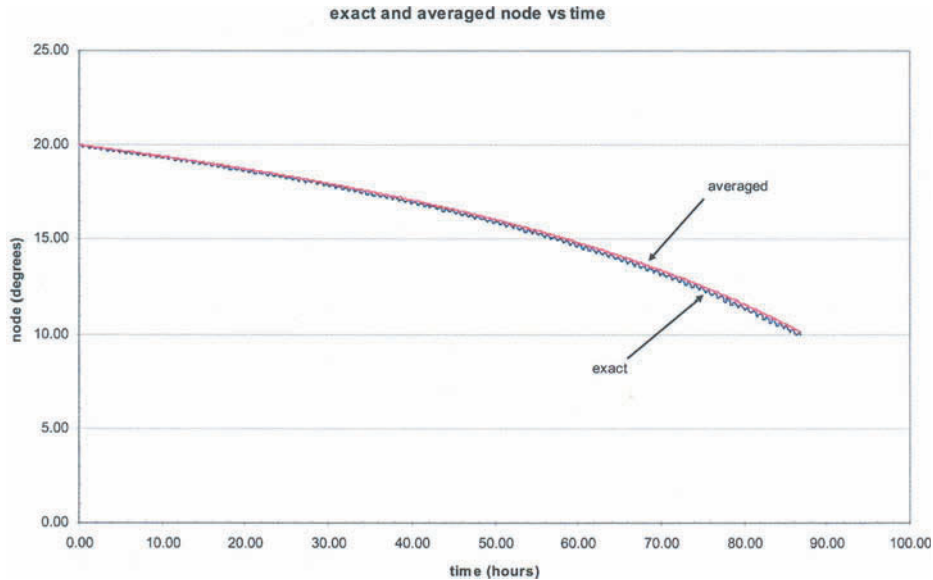


FIG. 5. Evolution of the Node for the Averaged and Exact Theories.

The terms with the T subscript depict the thrust acceleration parts, such that the Hamiltonian of this system is the sum of the thrust parts and the J_2 parts

$$\begin{aligned}
 H = 1 + \lambda_V \dot{V} + \lambda_i \dot{i} + \lambda_\Omega \dot{\Omega} + \lambda_\alpha \dot{\alpha} &= 1 + \lambda_V (-fc_\beta) + \lambda_i \left(\frac{fs_\beta c_\alpha}{V} \right) + \lambda_\Omega \left(\frac{fs_\beta s_\alpha}{Vs_i} \right) \\
 &+ \lambda_\alpha \left(\frac{V^3}{\mu} - \frac{fs_\beta s_\alpha}{V \tan i} \right) + \lambda_V \left[\frac{3J_2 R^2}{\mu^3} V^8 s_i^2 s_\alpha c_\alpha \right] + \lambda_i \left[-\frac{3J_2 R^2}{\mu^3} V^7 s_i c_i s_\alpha c_\alpha \right] \\
 &+ \lambda_\Omega \left[-\frac{3J_2 R^2}{\mu^3} V^7 c_i s_\alpha^2 \right] + \lambda_\alpha \left\{ \frac{3J_2 R^2}{\mu^3} V^7 [1 + s_\alpha^2 (1 - 4s_i^2)] \right\}
 \end{aligned} \quad (51)$$

The Euler-Lagrange equations are thus given by

$$\begin{aligned}
 \dot{\lambda}_V = -\frac{\partial H}{\partial V} &= \lambda_i \frac{fs_\beta c_\alpha}{V^2} + \lambda_\Omega \frac{fs_\beta s_\alpha}{V^2 s_i} - \lambda_\alpha \left(\frac{3V^2}{\mu} \right) - \lambda_\alpha \frac{fs_\beta s_\alpha}{V^2 \tan i} \\
 &- \lambda_V \left[\frac{3J_2 R^2}{\mu^3} 8V^7 s_i^2 s_\alpha c_\alpha \right] - \lambda_i \left[-\frac{3J_2 R^2}{\mu^3} 7V^6 s_i c_i s_\alpha c_\alpha \right] - \lambda_\Omega \left[-\frac{3J_2 R^2}{\mu^3} 7V^6 c_i s_\alpha^2 \right] \\
 &- \lambda_\alpha \left\{ \frac{3J_2 R^2}{\mu^3} 7V^6 [1 + s_\alpha^2 (1 - 4s_i^2)] \right\}
 \end{aligned} \quad (52)$$

$$\begin{aligned}
 \dot{\lambda}_i = -\frac{\partial H}{\partial i} &= \lambda_\Omega \frac{fs_\beta s_\alpha c_i}{Vs_i^2} - \lambda_\alpha \frac{fs_\beta s_\alpha}{Vs_i^2} - \lambda_V \left[\frac{3J_2 R^2}{\mu^3} V^8 2s_i c_i s_\alpha c_\alpha \right] \\
 &- \lambda_i \left[-\frac{3J_2 R^2}{\mu^3} V^7 (c_i^2 - s_i^2) s_\alpha c_\alpha \right] - \lambda_\Omega \left[\frac{3J_2 R^2}{\mu^3} V^7 s_i s_\alpha^2 \right] \\
 &- \lambda_\alpha \left[-\frac{3J_2 R^2}{\mu^3} V^7 8s_\alpha^2 s_i c_i \right]
 \end{aligned} \quad (53)$$

$$\dot{\lambda}_\Omega = -\frac{\partial H}{\partial \Omega} = 0 \quad (54)$$

$$\begin{aligned} \dot{\lambda}_\alpha &= -\frac{\partial H}{\partial \alpha} = \lambda_i \frac{fs_\beta s_\alpha}{V} - \lambda_\Omega \frac{fs_\beta c_\alpha}{Vs_i} + \lambda_\alpha \frac{fs_\beta c_\alpha}{V \tan i} \\ &\quad - \lambda_V \left[\frac{3J_2R^2}{\mu^3} V^8 s_i^2 (c_\alpha^2 - s_\alpha^2) \right] - \lambda_i \left[-\frac{3J_2R^2}{\mu^3} V^7 s_i c_i (c_\alpha^2 - s_\alpha^2) \right] - \lambda_\Omega \left[-\frac{3J_2R^2}{\mu^3} V^7 c_i 2s_\alpha c_\alpha \right] \\ &\quad - \lambda_\alpha \left[\frac{3J_2R^2}{\mu^3} V^7 2s_\alpha c_\alpha (1 - 4s_i^2) \right] \end{aligned} \quad (55)$$

The optimal firing angle β is once again given by the optimality condition $\frac{\partial H}{\partial \beta} = 0$ leading to

$$\tan \beta = \frac{-\lambda_i \frac{c_\alpha}{V} - \lambda_\Omega \frac{s_\alpha}{Vs_i} + \lambda_\alpha \frac{s_\alpha}{V \tan i}}{\lambda_V} = \frac{s_\beta}{c_\beta} \quad (56)$$

A search has been carried out to solve the same example transfer discussed in this paper while simultaneously optimizing the initial departure location α_0 as well as the arrival location α_f in order to arrive at the overall minimum-time solution. The value for J_2 is set at 1.08263×10^{-3} and a local minimum labeled Minimum #1 shown in Tables 3 and 4 is found. Hallman in reference [11] found that when solving precision-integrated minimum-time transfers with optimized initial and final locations on the initial and final orbits respectively, the existence of multiple local minima is a distinct possibility. Thus due to the sensitivity of the problem to both the initial and more importantly, final location, he ran a series of minimum-time solutions for nearby entry points on the final orbit, meaning that the final location α_f was held fixed each time and the transfer optimized and the minimum-time solution found while also optimizing the initial departure point. It is essential to fix the final location α_f as in cumulative radians measured from the starting point and not an angle between 0 and 360 degrees because the minima may occur on different final orbits and not necessarily on the same final one. In Table 4, α_f is thus left in radians such that the total number of revolutions is easily obtained by dividing by 2π . Essentially starting each time with a guessed $(\lambda_V)_0, (\lambda_i)_0, (\lambda_\Omega)_0, \alpha_0, (\lambda_\alpha)_0 = 0$ and a guessed value of t_f , the five search parameters namely $(\lambda_V)_0, (\lambda_i)_0, (\lambda_\Omega)_0, \alpha_0$, and t_f are searched and the dynamic and adjoint equations (47–50) and (52–55) are integrated numerically using the continuously varying β angle given by the optimality condition (56) until $V_f, i_f, \Omega_f, \alpha_f, H_f = 0$ are satisfied.

A nonlinear programming software called NLP2 developed at The Aerospace Corporation is used to carry out the searches with the constraints c_i driven to zero to within a small tolerance. Integration controls are set to the 10^{-16} level for both the relative and absolute errors. Thus at $t_f, c_1 = V - V_f, c_2 = i - i_f, c_3 = \Omega - \Omega_f, c_4 = \alpha - \alpha_f$ and $c_5 = H - H_f$ are driven to near zero by NLP2. While spanning a relatively large interval in α_f , Hallman found two other possible minima. Then a modified set of constraints was used to zero in on the two new minima by replacing $c_4 = \alpha - \alpha_f$ by $c_4 = \lambda_\alpha - (\lambda_\alpha)_f$ with $(\lambda_\alpha)_f = 0$ such that the optimal entry points on the final orbits are finally arrived at by searching once again on $(\lambda_V)_0, (\lambda_i)_0, (\lambda_\Omega)_0, \alpha_0$ and t_f with a guessed t_f that is retrieved from the set of the above-mentioned series of runs that corresponds to a local dip in the t_f values. This search

TABLE 3. Solutions From the Three Precision-Integrated Local Minima (Four-State Unaveraged) and the Averaged (Three-State with Piecewise-Constant Yaw)

	$(\lambda_v)_0$ (s/km/s)	$(\lambda_i)_0$ (s/rad)	$(\lambda_n)_0$ (s/rad)	α_0 (deg)	t_f (s)	ΔV (km/s)
Minimum #1	0.689315697×10^5	0.299691308×10^7	-0.178480579×10^6	-13.2309819	3.42012214×10^5	1.1970427
Minimum #2	0.288250837×10^6	0.750433878×10^7	-0.430366566×10^6	-34.388762	3.41673186×10^5	1.1958561
Minimum #3	0.1096211864×10^6	0.383795138×10^7	-0.224840404×10^6	-20.6460985	3.41282707×10^5	1.1944895
Averaged	0.546709224×10^6	0.214122398×10^8	-0.547250956×10^6	NA	3.88355734×10^5	1.3592451

TABLE 4. Initial and Final Achieved Parameters for the Three Precision-Integrated Local Minima (Four-State Unaveraged) and the Averaged (Three-State with Piecewise-Constant Yaw)

	V_0 (km/s)	i_0 (deg)	Ω_0 (deg)	α_0 (deg)	$(\lambda_a)_0$ (s/rad)	H_f
	V_f (km/s)	i_f (deg)	Ω_f (deg)	α_f (deg)	$(\lambda_a)_f$ (s/rad)	
Minimum #1	7.7931587	10.0	20.0	-13.2309819	0.0	
	7.6126915	4.99999815	9.99996333	386.639054	0.216353×10^{-5}	0.384556×10^{-5}
Minimum #2	7.7931587	10.0	20.0	-34.3887621	0.0	
	7.61269218	5.00000000	10.00000000	380.862035	-0.206772×10^{-5}	$-0.342145 \times 10^{-12}$
Minimum #3	7.7931587	10.0	20.0	-20.6460985	0.0	
	7.61269218	5.00000000	10.00000000	383.723086	-0.713620×10^{-6}	$-0.632865 \times 10^{-10}$
Averaged	7.7931587	10.0	20.0	NA	NA	
	7.6126751	4.99999999	9.99915629	NA	NA	-0.386454×10^{-4}

is now much easier to carry out because the value of α_f that needs to be optimized is already very close to the optimal value and in its immediate vicinity. Thus the other two minima are found as shown in Tables 3 and 4. The three minima are clustered to within about five minutes of each other in transfer time. Minimum #3 is clearly the global minimum for this example transfer. Note that the Hamiltonian, not being an explicit function of time, is constant throughout all three trajectories at the near-zero value. Also the $(\lambda_\alpha)_f$ values are near-zero for the optimized entry locations which differ only by about three radians in cumulative α values. The final V_f, i_f, Ω_f parameters are also clearly matched. Note that H is a constant of the motion, being independent of time. Minimum #1 was generated by using the algorithm UNCMIN of reference [12] which minimizes the sum of squares of the errors at t_f , while Minima #2 and 3 were generated by NLP2 resulting in more resolution as seen by the values of H_f in Table 4.

The Three-State Averaged System with J_2

It is well known that the secular perturbations of the first order do not affect the mean values of a , e , and i . For example

$$\dot{(\bar{i})}_{J_2} = \frac{1}{2\pi} \int_0^{2\pi} (\dot{i})_{J_2} d\alpha = \frac{1}{2\pi} \int_0^{2\pi} \frac{(f_h)_{J_2} c_\alpha}{V} d\alpha = -\frac{1}{2\pi} \frac{3J_2 R^2}{\mu^3} V^7 s_i c_i \int_0^{2\pi} s_\alpha c_\alpha d\alpha = 0$$

However

$$\begin{aligned} \dot{(\bar{\Omega})}_{J_2} &= \frac{1}{2\pi} \int_0^{2\pi} (\dot{\Omega})_{J_2} d\alpha = \frac{1}{2\pi} \int_0^{2\pi} \frac{(f_h)_{J_2} s_\alpha}{Vs_i} d\alpha \\ &= -\frac{3}{2\pi} \frac{J_2 R^2}{\mu^3} V^7 c_i \int_0^{2\pi} s_\alpha^2 d\alpha = -\frac{3}{2} \frac{J_2 R^2}{\mu^3} V^7 c_i \end{aligned} \quad (57)$$

which leads us to the following system of three equations for V , i and Ω , while neglecting the $\dot{\omega}$ and \dot{M} equations

$$\dot{\bar{V}} = -fc_\beta \quad (58)$$

$$\dot{\bar{i}} = \frac{2fs_\beta}{\pi V} c_{\theta_{c_n}} \quad (59)$$

$$\dot{\bar{\Omega}} = \frac{2fs_\beta}{\pi Vs_i} s_{\theta_{c_n}} - \frac{3}{2} \frac{J_2 R^2}{\mu^3} V^7 c_i \quad (60)$$

The use of the mean elements effectively neglects the short peiod perturbations due to J_2 . This assumption is even more valid as the thrust level decreases.

As in the first section, θ_c is the instantaneous angular position of the relative line of nodes which is now being perturbed due to the Ω precession induced by J_2 . Thus the thrust averaging holds the β angle piecewise constant switching signs at the relative antinodes, i.e., ± 90 deg away from θ_c , the latter depicted now by θ_{c_n} in Figure 1. It is thus also necessary to update the value of θ_f depicted by θ_{f_n} because it is no longer constant. The instantaneous orbit orientation is now defined by Ω_n and i_n as these quantities are being integrated numerically. The relative inclination i_n^* of the instantaneous orbit with respect to the final orbit is given by

$$c_{i_n^*} = c_{\Omega_n - \Omega_2} s_{i_n} s_{i_2} + c_{i_n} c_{i_2} \quad (61)$$

If $\Omega_n < \Omega_f$ during integration, then from spherical trigonometry

$$s_{\theta_{f_n}} = s_{i_n} s_{\Omega_2 - \Omega_n} / s_{i_n^*} \quad (62)$$

$$c_{\theta_{f_n}} = (c_{i_n} - c_{i_2} c_{i_n^*}) / (s_{i_2} s_{i_n^*}) \quad (63)$$

which allows us to update θ_{c_n} from

$$s_{\theta_{c_n}} = s_{i_2} s_{\Omega_2 - \Omega_n} / s_{i_n^*} \quad (64)$$

$$c_{\theta_{c_n}} = c_{\Omega_2 - \Omega_n} c_{\theta_{f_n}} - s_{\Omega_2 - \Omega_n} s_{\theta_{f_n}} c_{i_2} \quad (65)$$

If $\Omega_n > \Omega_f$ during integration, then θ_{f_n} and θ_{c_n} are obtained from

$$s_{\theta_{f_n}} = s_{i_n} s_{\Omega_n - \Omega_2} / s_{i_n^*} \quad (66)$$

$$c_{\theta_{f_n}} = (c_{i_n^*} c_{i_2} - c_{i_n}) / (s_{i_n^*} s_{i_2}) \quad (67)$$

$$s_{\theta_{c_n}} = s_{i_2} s_{\Omega_n - \Omega_2} / s_{i_n^*} \quad (68)$$

$$c_{\theta_{c_n}} = c_{\theta_{f_n}} c_{\Omega_n - \Omega_2} + s_{\theta_{f_n}} s_{\Omega_n - \Omega_2} c_{i_2} \quad (69)$$

This reduced three-state dynamics accepts now the following averaged Hamiltonian

$$\begin{aligned} \tilde{H} = 1 + \tilde{\lambda}_V \dot{\tilde{V}} + \tilde{\lambda}_i \dot{\tilde{i}} + \tilde{\lambda}_\Omega \dot{\tilde{\Omega}} &= 1 - \tilde{\lambda}_V f c_\beta + \tilde{\lambda}_i \frac{2 f s_\beta}{\pi \tilde{V}} c_{\theta_{c_n}} \\ &+ \tilde{\lambda}_\Omega \left(\frac{2 f s_\beta}{\pi \tilde{V} s_i} s_{\theta_{c_n}} \right) + \tilde{\lambda}_\Omega \left[-\frac{3}{2} \frac{J_2 R^2}{\mu^3} \tilde{V}^7 c_{\tilde{i}} \right] \end{aligned} \quad (70)$$

leading to the adjoints

$$\dot{\tilde{\lambda}}_V = -\partial \tilde{H} / \partial \tilde{V} = \frac{2 f s_\beta}{\pi \tilde{V}^2} \left(\tilde{\lambda}_i c_{\theta_{c_n}} + \frac{\tilde{\lambda}_\Omega}{s_{\tilde{i}}} s_{\theta_{c_n}} \right) + \tilde{\lambda}_\Omega \frac{3}{2} \frac{J_2 R^2}{\mu^3} 7 \tilde{V}^6 c_{\tilde{i}} \quad (71)$$

$$\dot{\tilde{\lambda}}_i = -\partial \tilde{H} / \partial \tilde{i} = \tilde{\lambda}_\Omega \frac{2 f s_\beta}{\pi \tilde{V}} \frac{c_{\tilde{i}}}{s_{\tilde{i}}^2} s_{\theta_{c_n}} - \tilde{\lambda}_\Omega \left(\frac{3}{2} \frac{J_2 R^2}{\mu^3} \tilde{V}^7 s_{\tilde{i}} \right) \quad (72)$$

$$\dot{\tilde{\lambda}}_\Omega = -\partial \tilde{H} / \partial \tilde{\Omega} = 0 \quad (73)$$

The firing angle is given by the optimality condition $\partial \tilde{H} / \partial \beta = 0$ leading to

$$\tan \beta = -\left(\dot{\tilde{\lambda}}_i c_{\theta_{c_n}} + \frac{\tilde{\lambda}_\Omega}{s_{\tilde{i}}} s_{\theta_{c_n}} \right) \frac{2}{\pi \tilde{V} \tilde{\lambda}_V} = \frac{s_\beta}{c_\beta} \quad (74)$$

Thus equations (58–60) and (71–73) constitute the set of dynamic and adjoints equations to integrate simultaneously by using the optimal β angle in equation (74). The search now consists of $(\tilde{\lambda}_V)_0$, $(\tilde{\lambda}_i)_0$, $(\tilde{\lambda}_\Omega)_0$, as well as t_f such that starting from \tilde{V}_0 , \tilde{i}_0 , $\tilde{\Omega}_0$, the final values \tilde{V}_f , \tilde{i}_f , $\tilde{\Omega}_f$ are matched as well as $\tilde{H}_f = 0$. The solution is shown in Tables 3 and 4 under the label “Averaged.” This optimization problem is much easier to solve than the corresponding precision-integration problem of the previous section and it visibly has a single local minimum within the timeframe t_f associated with the cases discussed thus far, as the clustered minima vanish due to the averaging. Note that t_f is now about some 13.79% larger than that corresponding to the global precision-integrated Minimum #3. Equivalently the ΔV required for the transfer is equally larger by the same percentage. However the use of piecewise-constant β thrust yaw angle is much easier to implement in an operational

sense than the continuously varying thrust vector orientation needed to implement the unaveraged transfer. Figure 6 shows the θ_{c_n} and θ_{f_n} angles variations from $(\theta_{c_n})_0 = 9.7086461$ deg, $(\theta_{f_n})_0 = 19.6329215$ deg to the essentially common final value of $(\theta_{c_n})_f = 89.9978957$ deg $(\theta_{f_n})_f = 89.9970552$ deg. Also i_n^* decreases monotonically from $(i^*)_0 = 5.1489398$ deg to $(i^*)_f = 0.73534 \times 10^{-4}$ or effectively zero as the current orbit merges with the final target orbit. Figures 7 and 8 show the variation in inclination for the three “exact” trajectories as well as the “averaged” one with the latter curve smooth without any of the small fluctuations shown on the “exact” ones. Note that Minimum #2 shows the largest decrease in velocity during the actual transfer meaning that the orbit expands to a larger size before shrinking back towards its target size. A very small similar effect is noted near the trajectory end for the “averaged” transfer.

In Fig. 9, the node Ω wanders beyond the final Ω_f of 10 deg before reversing course and reaching the target 10 deg mark. This wander is very large for the “averaged” transfer and is responsible for the corresponding longer flight time. This large deviation is due to the strategy adopted by the “averaged” transfer consisting of rotating the current orbit around the current line of nodes of the current and final orbits as this is not necessarily very efficient because “unwanted” Ω changes are being generated besides the J_2 -induced Ω change itself. That is why Ω decreases much more rapidly than desired. However the rotation strategy will eventually achieve the final orbit because the wedge angle will be driven to zero in time. Note that the inclination curve in Fig. 7 stays rather close to the “exact” ones. A large scale parametric study involving orbit size and orientation as well as thrust acceleration may reveal the favorable and the less favorable regions where this particular averaging strategy would be more or less desirable to implement without recurring significant penalties in total transfer time.

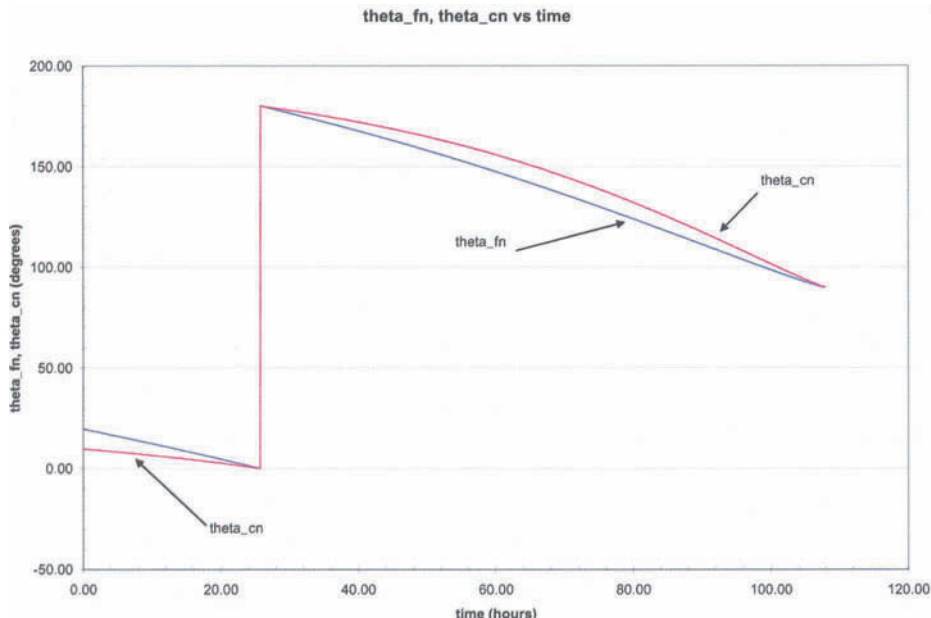


FIG. 6. Evolution of the θ_{c_n} and θ_{f_n} Angular Position Angles for the J_2 -Perturbed Averaged Theory.

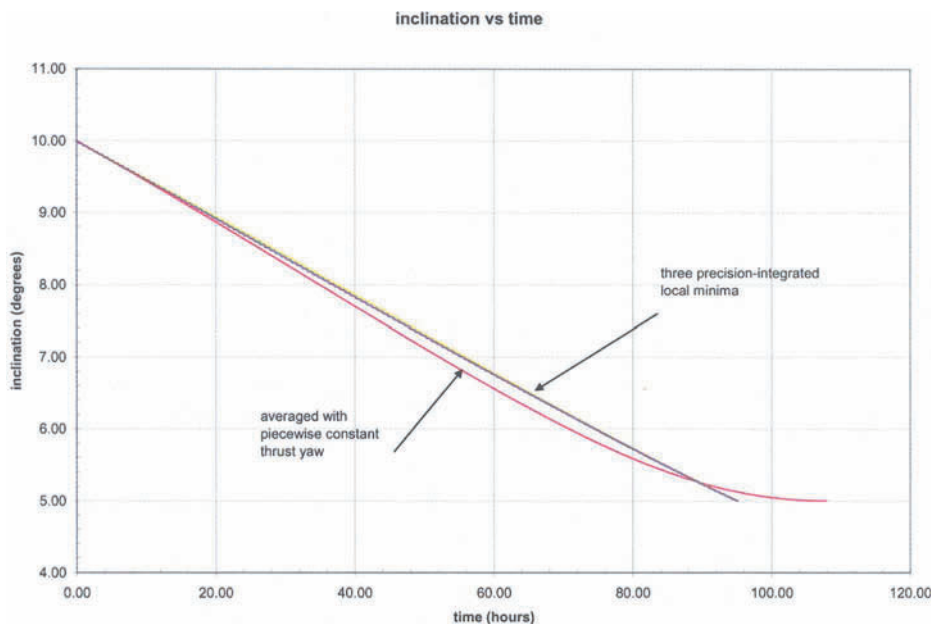


FIG. 7. Inclination Variation for the Three Exact Local Minima and the Averaged Transfer Under J_2 Influence.

Figure 10 shows the last few hours of the “exact” transfers as far as (λ_α) is concerned with high frequency oscillations crossing the zero value multiple times making the enforcement of $(\lambda_\alpha)_f = 0$ problematic especially when all three curves end

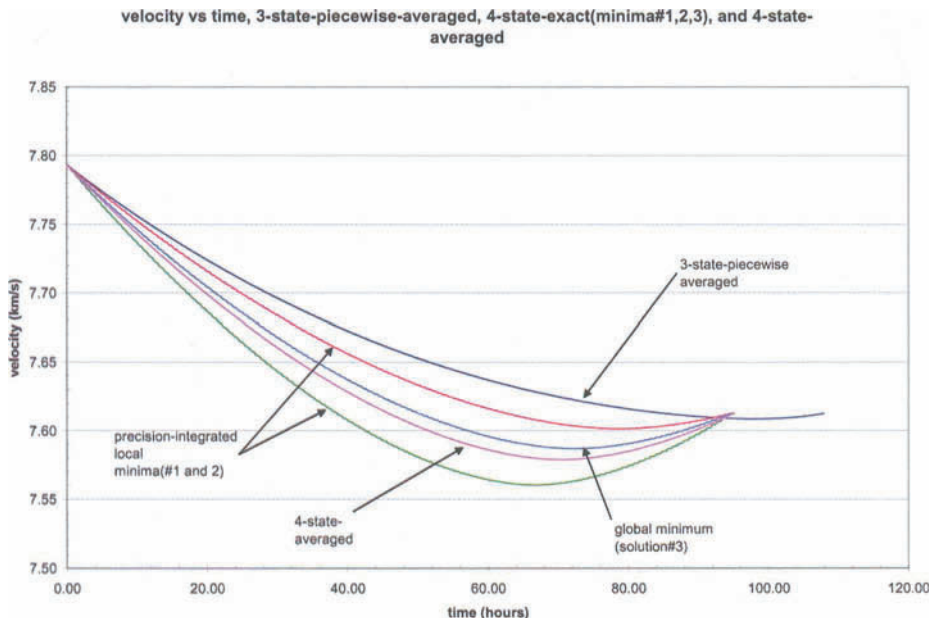


FIG. 8. Velocity Variation for the Three Exact Local Minima and the Averaged Transfer Under J_2 Influence.

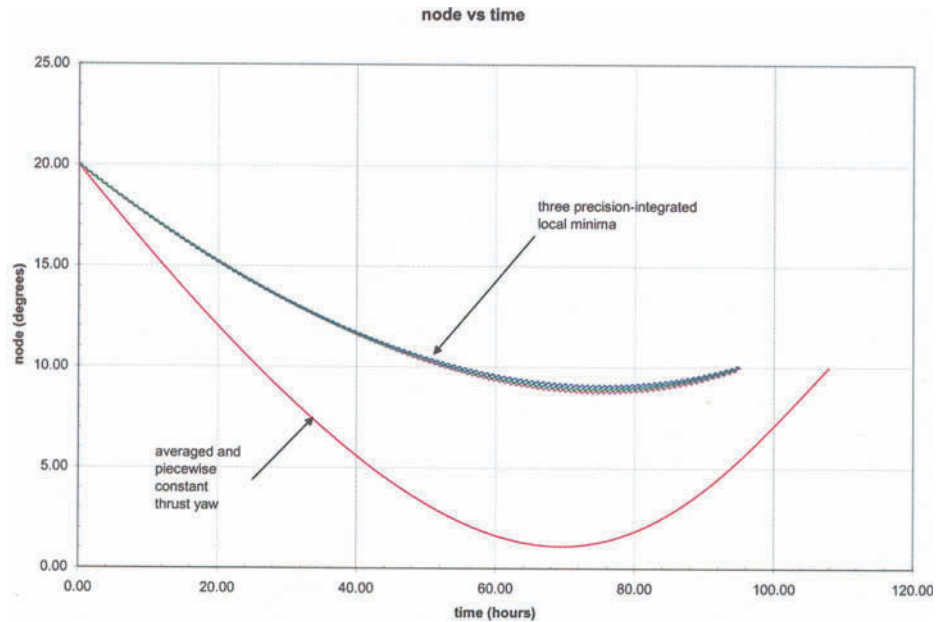


FIG. 9. Node Variation for the Three Exact Local Minima and the Averaged Transfer Under J_2 Influence.

at zero so close to one another. In Fig. 11, the continuously varying β angle for all three minima exhibit a complex behavior near the trajectory ends which could make the thrust vector orientation control difficult to implement. Figures 12 and 13 show the small fluctuations in the inclination and node mentioned earlier on a scale

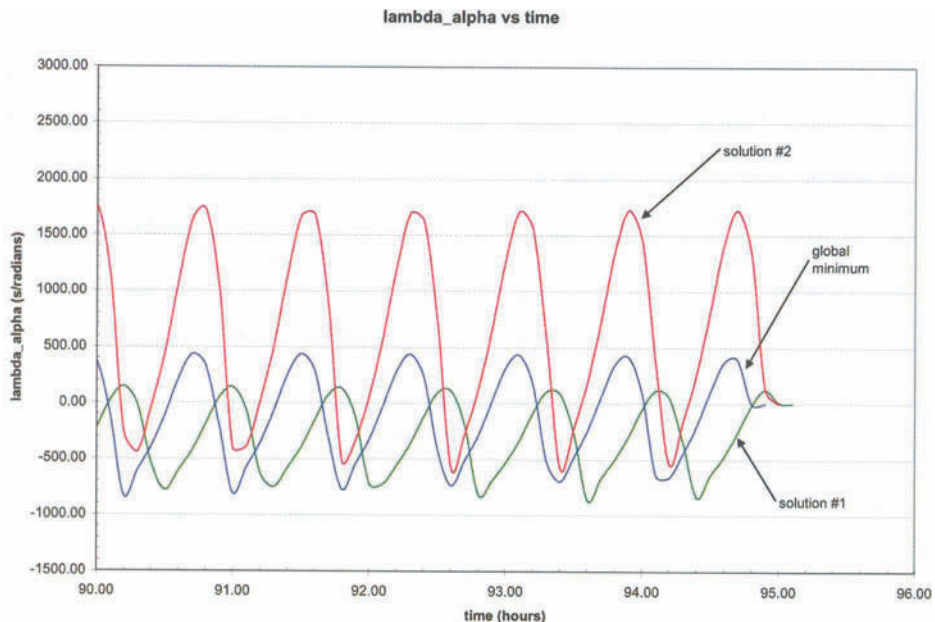


FIG. 10. Evolution of λ_α for the Three Local Minima Under J_2 Influence During Last Phase of Transfers.

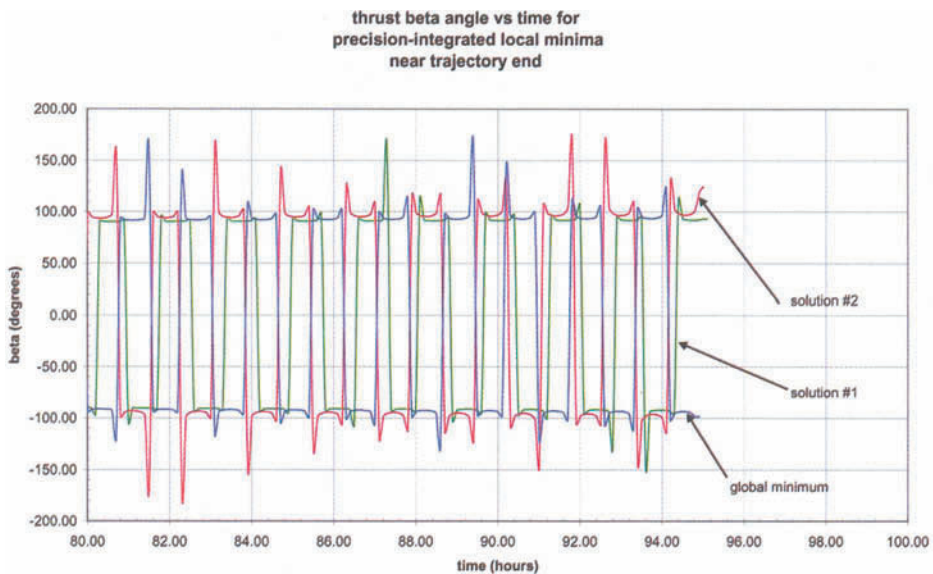


FIG. 11. Thrust β Angle Histories for the Three Local Minima Under J_2 Influence During Last Phase of Transfers.

that is easily visible near the point where the trajectory ends. The small difference in flight times is clearly visible as i and Ω reach their target values of 5 and 10 deg respectively. Finally, Fig. 14 shows the β angle history of the global minimum “exact” solution with the complex pattern shown near the end as discussed in Fig. 11, and the much smoother β angle history of the “averaged” solution which effectively

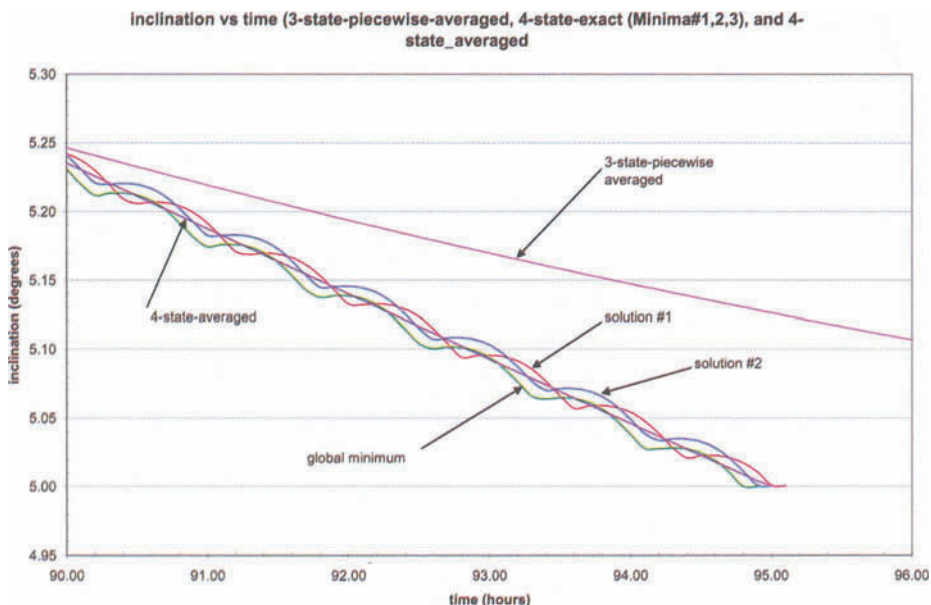


FIG. 12. Inclination Variation for the Three Local Minima Under J_2 Influence During Last Phase of Transfers.

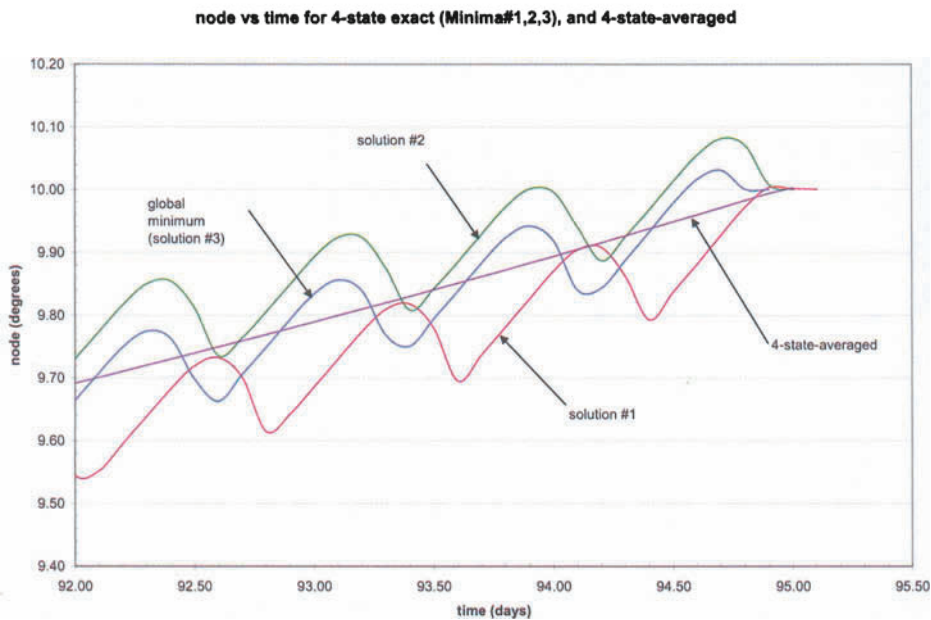


FIG. 13. Node Variation for the Three Local Minima Under J_2 Influence During Last Phase of Transfers.

changes sign at the antinodes within each orbit. As for the thrust-only averaged case, the Hamiltonian \tilde{H} is not constant because of the formulation involving the angle θ_c . The Hamiltonian \tilde{H} decreases from -4.20434 at time zero to about -4.55239 at $t = 44.4$ hrs and then increases in a parabolic manner until $\tilde{H} \approx 0$ at t_f .

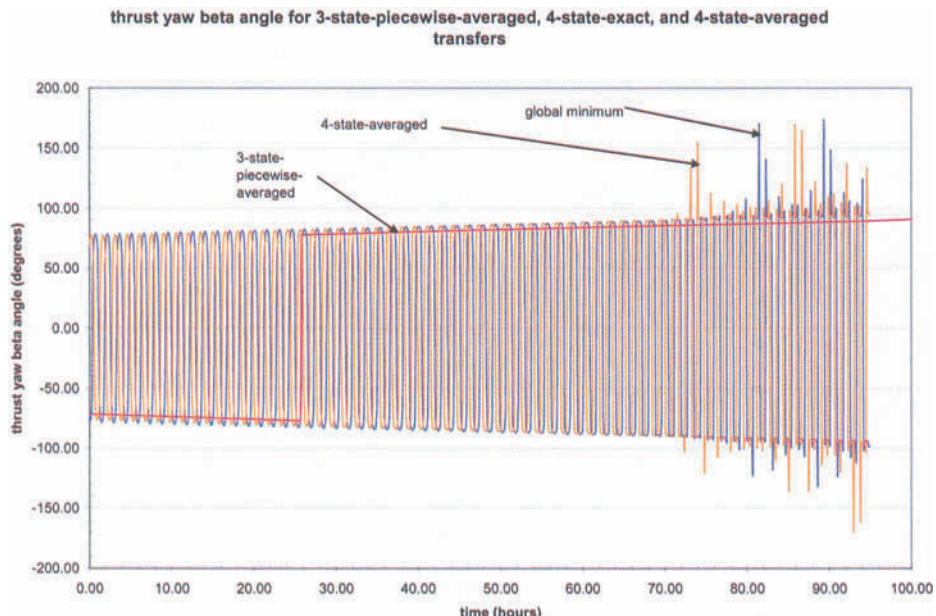


FIG. 14. Thrust β Angle for the Global Minimum and the Averaged Transfers Under J_2 Influence.

Several of the plots shown in this paper can also be depicted as a function of running orbit number. For example, equation (11) for the angular position θ can be integrated by using $n = V^3/\mu$ with V given as a function of time t in reference [4]. However these plots are left as they are for easier interpretation.

Averaging of the J_2 -Perturbed Four-State Dynamics using Numerical Quadrature

Going back to equations (47–50) for $\dot{V}, \dot{i}, \dot{\Omega}$ and $\dot{\alpha}$ the averaged Hamiltonian can be written as

$$\tilde{H} = \frac{1}{T_0} \int_0^{T_0} H dt = \frac{1}{T_0} \int_{-\pi}^{\pi} \frac{H d\alpha}{\dot{\alpha}(\tilde{z}, \alpha)} \quad (75)$$

with H given by equation (51), and with $\tilde{z} = (\tilde{V} \ \tilde{i} \ \tilde{\Omega} \ \tilde{\alpha})^T$ standing for the state vector, and T_0 for the orbit period given by $T_0 = 2\pi/\tilde{n}$. From Kepler's equation and in view of $\tilde{r} = \tilde{a}$, the circular orbit assumption, $\tilde{n} = \dot{E} = \dot{\alpha} = \frac{V^3}{\mu}$ where E is the eccentric anomaly in Kepler's equation $\tilde{M} = E - \tilde{e}s_E = \tilde{n}t$. Thus

$$\tilde{H} = \frac{1}{2\pi} \int_{-\pi}^{\pi} H d\alpha \quad (76)$$

leading to the state and adjoint equations

$$\dot{\tilde{z}} = \partial \tilde{H} / \partial \tilde{\lambda}_z = \frac{1}{2\pi} \int_{-\pi}^{\pi} \left(\frac{\partial H}{\partial \tilde{\lambda}_z} \right)^T d\alpha \quad (77)$$

$$\dot{\tilde{\lambda}}_z = -(\partial \tilde{H} / \partial \tilde{z})^T = -\frac{1}{2\pi} \int_{-\pi}^{\pi} \left(\frac{\partial H}{\partial \tilde{z}} \right)^T d\alpha \quad (78)$$

such that the averaged state derivatives are obtained by quadrature from

$$\dot{\tilde{V}} = \frac{1}{2\pi} \int_{-\pi}^{\pi} \dot{V} d\alpha = \frac{1}{2\pi} \int_{-\pi}^{\pi} \left(-f c_\beta + \frac{3J_2 R^2}{\mu^3} V^8 s_i^2 s_\alpha c_\alpha \right) d\alpha \quad (79)$$

$$\dot{\tilde{i}} = \frac{1}{2\pi} \int_{-\pi}^{\pi} \dot{i} d\alpha = \frac{1}{2\pi} \int_{-\pi}^{\pi} \left(\frac{f s_\beta c_\alpha}{V} - \frac{3J_2 R^2}{\mu^3} V^7 s_i c_i s_\alpha c_\alpha \right) d\alpha \quad (80)$$

$$\dot{\tilde{\Omega}} = \frac{1}{2\pi} \int_{-\pi}^{\pi} \dot{\Omega} d\alpha = \frac{1}{2\pi} \int_{-\pi}^{\pi} \left(\frac{f s_\beta s_\alpha}{V s_i} - \frac{3J_2 R^2}{\mu^3} V^7 c_i s_\alpha^2 \right) d\alpha \quad (81)$$

$$\dot{\tilde{\alpha}} = \frac{1}{2\pi} \int_{-\pi}^{\pi} \dot{\alpha} d\alpha = \frac{1}{2\pi} \int_{-\pi}^{\pi} \left\{ \frac{V^3}{\mu} - \frac{f s_\beta s_\alpha}{V \tan i} + \frac{3J_2 R^2 V^7}{\mu^3} [1 + s_\alpha^2(1 - 4s_i^2)] \right\} d\alpha \quad (82)$$

In a similar way, the averaged adjoint derivatives are obtained from

$$\begin{aligned} \dot{\tilde{\lambda}}_V &= \frac{1}{2\pi} \int_{-\pi}^{\pi} \dot{\lambda}_V d\alpha = \frac{1}{2\pi} \int_{-\pi}^{\pi} \left\{ \frac{\lambda_i f s_\beta c_\alpha}{V^2} + \frac{\lambda_\Omega f s_\beta s_\alpha}{V^2 s_i} - \lambda_\alpha \frac{3V^2}{\mu} - \lambda_\alpha \frac{f s_\beta s_\alpha}{V^2 \tan i} \right. \\ &\quad \left. - \lambda_V \left[\frac{3J_2 R^2}{\mu^3} 8V^7 s_i^2 s_\alpha c_\alpha \right] - \lambda_i \left[-\frac{3J_2 R^2}{\mu^3} 7V^6 s_i c_i s_\alpha c_\alpha \right] - \lambda_\Omega \left[-\frac{3J_2 R^2}{\mu^3} 7V^6 c_i s_\alpha^2 \right] \right. \\ &\quad \left. - \lambda_\alpha \left[\frac{3J_2 R^2}{\mu^3} 7V^6 [1 + s_\alpha^2(1 - 4s_i^2)] \right] \right\} d\alpha \end{aligned} \quad (83)$$

$$\begin{aligned}\dot{\lambda}_i &= \frac{1}{2\pi} \int_{-\pi}^{\pi} \dot{\lambda}_i d\alpha = \frac{1}{2\pi} \int_{-\pi}^{\pi} \left\{ \frac{\lambda_\Omega f s_\beta c_i s_\alpha}{V s_i^2} - \frac{\lambda_\alpha f s_\beta s_\alpha}{V s_i^2} - \lambda_v \left[\frac{3J_2 R^2}{\mu^3} V^8 2 s_i c_i s_\alpha c_\alpha \right] \right. \\ &\quad \left. - \lambda_i \left[-\frac{3J_2 R^2}{\mu^3} V^7 c_{2i} s_\alpha c_\alpha \right] - \lambda_\Omega \left[\frac{3J_2 R^2}{\mu^3} V^7 s_i s_\alpha^2 \right] - \lambda_\alpha \left[-\frac{3J_2 R^2}{\mu^3} V^7 8 s_i c_i s_\alpha^2 \right] \right\} d\alpha \quad (84)\end{aligned}$$

$$\dot{\lambda}_\Omega = \frac{1}{2\pi} \int_{-\pi}^{\pi} \dot{\lambda}_\Omega d\alpha = 0 \quad (85)$$

$$\begin{aligned}\dot{\lambda}_\alpha &= \frac{1}{2\pi} \int_{-\pi}^{\pi} \dot{\lambda}_\alpha d\alpha = \frac{1}{2\pi} \int_{-\pi}^{\pi} \left\{ \frac{\lambda_i f s_\beta s_\alpha}{V} - \frac{\lambda_\Omega f s_\beta c_\alpha}{V s_i} + \frac{\lambda_\alpha f s_\beta c_\alpha}{V \tan i} - \lambda_v \left[\frac{3J_2 R^2}{\mu^3} V^8 s_i^2 c_{2\alpha} \right] \right. \\ &\quad \left. - \lambda_i \left[-\frac{3J_2 R^2}{\mu^3} V^7 s_i c_i c_{2\alpha} \right] - \lambda_\Omega \left[-\frac{3J_2 R^2}{\mu^3} V^7 c_i 2 s_\alpha c_\alpha \right] \right. \\ &\quad \left. - \lambda_\alpha \left[\frac{3J_2 R^2}{\mu^3} V^7 (1 - 4 s_i^2) 2 s_\alpha c_\alpha \right] \right\} d\alpha \quad (86)\end{aligned}$$

The optimal firing angle β is given by

$$\tan \beta = \frac{-\frac{\tilde{\lambda}_i c_{\tilde{\alpha}}}{\tilde{V}} - \frac{\tilde{\lambda}_\Omega s_{\tilde{\alpha}}}{\tilde{V} s_i} + \frac{\tilde{\lambda}_\alpha \tilde{s}_\alpha}{\tilde{V} \tan \tilde{i}}}{\tilde{\lambda}_v} = \frac{s_\beta}{c_\beta} \quad (87)$$

It is clear that β is continuously varying and that the J_2 terms in $\dot{\tilde{V}}$ and $\dot{\tilde{i}}$ involving $s_\alpha c_\alpha$ will not contribute and can be safely dropped. The same is true for the $s_\alpha c_\alpha$ terms in $\dot{\tilde{\lambda}}_v$, $\dot{\tilde{\lambda}}_i$, and $\dot{\tilde{\lambda}}_\alpha$ integrals. Also, the $c_{2\alpha}$ terms in $\dot{\tilde{\lambda}}_\alpha$ can be dropped for the same reason.

Because the β angle is associated with the thrust terms and not the J_2 terms in equations (79–86), the averaging out of the angular position α from the J_2 terms can be carried out analytically without the need for numerical quadrature. The $s_\alpha c_\alpha$ terms will not contribute while the s_α^2 terms will contribute π from the integrations such that these equations simplify to the set given by

$$\dot{\tilde{V}} = \frac{1}{2\pi} \int_{-\pi}^{\pi} -f c_\beta d\alpha \quad (88)$$

$$\dot{\tilde{i}} = \frac{1}{2\pi} \int_{-\pi}^{\pi} \frac{f s_\beta c_\alpha}{V} d\alpha \quad (89)$$

$$\dot{\tilde{\Omega}} = \frac{1}{2\pi} \int_{-\pi}^{\pi} \frac{f s_\beta s_\alpha}{V s_i} d\alpha - \frac{3}{2} \frac{J_2 R^2}{\mu^3} V^7 c_i \quad (90)$$

$$\dot{\tilde{\alpha}} = \frac{1}{2\pi} \int_{-\pi}^{\pi} \left(\frac{V^3}{\mu} - \frac{f s_\beta s_\alpha}{V \tan i} \right) d\alpha + \frac{3J_2 R^2}{\mu^3} V^7 \left(\frac{3}{2} - 2 s_i^2 \right) \quad (91)$$

$$\dot{\tilde{\lambda}}_i = \frac{1}{2\pi} \int_{-\pi}^{\pi} \left(\frac{\lambda_\Omega f s_\beta s_\alpha c_i}{V s_i^2} - \frac{\lambda_\alpha f s_\beta s_\alpha}{V s_i^2} \right) d\alpha + \frac{3}{2} \frac{J_2 R^2}{\mu^3} V^7 (-\lambda_\Omega s_i + 8 \lambda_\alpha s_i c_i) \quad (92)$$

$$\begin{aligned}\dot{\tilde{\lambda}}_v &= \frac{1}{2\pi} \int_{-\pi}^{\pi} \left(\frac{\lambda_i f s_\beta c_\alpha}{V^2} + \frac{\lambda_\Omega f s_\beta s_\alpha}{V^2 s_i} - \lambda_\alpha \frac{3V^2}{\mu} - \lambda_\alpha \frac{f s_\beta s_\alpha}{V^2 \tan i} \right) d\alpha \\ &\quad + \frac{3}{2} \frac{J_2 R^2}{\mu^3} 7V^6 [\lambda_\Omega c_i - \lambda_\alpha (3 - 4s_i^2)]\end{aligned}\quad (93)$$

$$\dot{\tilde{\lambda}}_\Omega = 0 \quad (94)$$

$$\dot{\tilde{\lambda}}_\alpha = \frac{1}{2\pi} \int_{-\pi}^{\pi} \left(\lambda_i \frac{f s_\beta s_\alpha}{V} - \frac{\lambda_\Omega f s_\beta c_\alpha}{V s_i} + \lambda_\alpha \frac{f s_\beta c_\alpha}{V \tan i} \right) d\alpha \quad (95)$$

When J_2 is turned off, \tilde{H} being a constant of the motion due to the fact that it is not an explicit function of time, is effectively staying constant with a relatively small number of segments of the order of 16 needed to carry out the eight-point Legendre-Gauss quadrature in this particular example of relatively high acceleration $f = 3.5 \times 10^{-6}$ km/s². However when J_2 is on, the β history which is basically oscillatory in the beginning of the trajectory, becomes more complicated near the end as shown in Fig. 14 for the “exact” case. The transition from the purely oscillatory mode to the more complicated one challenges the constancy of \tilde{H} during that period, requiring a large number of segments of the order of 128 and higher for the quadrature to force \tilde{H} to remain also constant during the transition period, making the numerical integrations more time-consuming. This difficulty may be the result of using relatively high thrust accelerations combined with J_2 while dwelling in the LEO environment. The following solution is found, namely $(\lambda_v)_0 = 0.140168691 \times 10^6$ s/km/s, $(\lambda_i)_0 = 0.445773755 \times 10^7$ s/rad, $(\lambda_\Omega)_0 = -0.259177663 \times 10^6$ s/rad, $\alpha_0 = 112.007934$ deg, $(\lambda_\alpha)_f = -0.406767769 \times 10^{-7}$ s/rad, $H_f = -0.148932970 \times 10^{-3}$, $t_f = 0.341928948 \times 10^6$ s, and the achieved parameters $V_f = 7.61252604$ km/s, $i_f = 5.000040$ deg, $\Omega_f = 10.002697$ deg, and $\alpha_f = 385.990903$ deg. Figure 8 shows the velocity variation, closely following the one corresponding to the “exact” global minimum, while Figs. 12 and 13 show the corresponding inclination and node variations without the oscillations that are present in the “exact” local minima. Finally, Fig. 14 shows the β history of the four-state averaged case with the transition taking place a little earlier than for the precision-integrated global minimum transfer.

Conclusion

The technique of analytic averaging of the dynamic equations needed to solve optimal transfer problems between general circular orbits using low-thrust acceleration is revisited within the context of a reduced set of state variables which includes the right ascension of the ascending node Ω for further extension to the most relevant problem of the perturbed motion due to J_2 . Edelbaum’s results are thus recovered for the thrust-only case by way of numerical integration, and compared with an “exact” solution involving four state variables with unaveraged dynamics that keeps the angular position in the system equations, and which allows for fully optimized thrust vectoring. The analysis is further extended to the important J_2 -perturbed case by also considering both the analytic averaging of the system dynamics also removing the angular position variable from the system equations, and the

full unaveraged system involving all four relevant state variables and continuously optimized thrust vectoring during the transfer. Numerical comparisons on a transfer example show that for the real-world thrust-and- J_2 -perturbation case, the analytic averaging is about 13% less economical to carry out from a purely ΔV point-of-view, but much more easily implemented in actual operations because the thrust vector orientation keeps a constant direction with respect to rotating axes, unlike the “exact” case in which this orientation must be continuously steered in time. The existence of multiple minima in the precision-integrated case without the analytic averaging complicates the search even further as shown by an example. Further investigations spanning significant portions of the parametric space involving orbit size and orientation could reveal the regions where the averaged transfer solutions are truly even more competitive in ΔV with the “exact” transfers.

References

- [1] EDELBAUM, T.N. “Propulsion Requirements for Controllable Satellites,” *ARS Journal*, August 1961, pp. 1079–1089.
- [2] EDELBAUM, T.N. “Theory of Maxima and Minima,” *Optimization Techniques with Applications to Aerospace Systems*, edited by G. Leitmann, Academic, New York, 1962, pp. 1–32.
- [3] WIESEL, W.E. and ALFANO, S. “Optimal Many-Revolution Orbit Transfer,” presented as paper AAS 83-352 at the AAS/AIAA Astrodynamics Specialist Conference, Lake Placid, NY, August 1983.
- [4] KÉCHICHIAN, J.A. “Reformulation of Edelbaum’s Low-Thrust Transfer Problem Using Optimal Control Theory,” *Journal of Guidance, Control, and Dynamics*, Vol. 20, No. 5, September–October 1997.
- [5] KÉCHICHIAN, J.A. “Optimal Altitude-Constrained Low-Thrust Transfer Between Inclined Circular Orbits,” *Proceedings of the Malcolm D. Shuster Astronautics Symposium*, Grand Island, New York, June 13–15, 2005.
- [6] BRYSON, A.E. and HO, Y-C. *Applied Optimal Control*, Ginn and Company, Waltham, Massachusetts, 1969, pp. 117–127.
- [7] EDELBAUM, T.N., SACKETT, L.L., and MALCHOW, H.L. “Optimal Low-Thrust Geocentric Transfer,” presented as paper AIAA 73-1074 at the AIAA Electric Propulsion Conference, November 1973.
- [8] KÉCHICHIAN, J.A. “Minimum-Time Constant Acceleration Orbit Transfer with First-Order Oblateness Effect,” *Journal of Guidance, Control, and Dynamics*, Vol. 23, No. 4, July–August 2000, pp. 595–603.
- [9] KÉCHICHIAN, J.A. “The Streamlined and Complete Set of the Nonsingular J_2 -Perturbed Dynamic and Adjoint Equations for Trajectory Optimization in Terms of Eccentric Longitude,” presented as paper AAS 07-120 at the AAS/AIAA Space Flight Mechanics Meeting, Sedona, Arizona, January 28–31, 2007.
- [10] KÉCHICHIAN, J.A. “The Inclusion of the Higher Order J_3 and J_4 Zonal Harmonics in the Modelling of Optimal Low-Thrust Orbit Transfer,” presented as paper AAS 08-198 at the AAS/AIAA Space Flight Mechanics Meeting, Galveston, Texas, January 27–31, 2008.
- [11] HALLMAN, W.P. personal communication, 2008.
- [12] KAHANER, D., MOLER, C., and NASH, S. *Numerical Methods and Software*, Prentice Hall, Englewood Cliffs, NJ, 1989.